

Should $\Delta\Sigma$ Modulators Used in AC Motor Drives be Adapted to the Mechanical Load of the Motor?

Sergio Callegari
University of Bologna,
ARCES/DEIS, Italy
sergio.callegari@unibo.it

Federico Bizzarri
Polytechnic of Milan
DEI, Italy
bizzarri@elet.polimi.it

Abstract—We consider the use of $\Delta\Sigma$ modulators in ac motor drives, focusing on the many additional degrees of freedom that this option offers over Pulse Width Modulation (PWM). Following some recent results, we show that it is possible to fully adapt the $\Delta\Sigma$ modulator Noise Transfer Function (NTF) to the rest of the drive chain and that the approach can be pushed even to a fine adaptation of the NTF to the specific motor loading condition. We investigate whether and to what extent the adaptation should be pursued. Using a representative test case and extensive simulation, we conclude that a mild adaptation can be beneficial, leading to Signal to Noise Ratio (SNR) improvements in the order of a few dB, while the advantage pushing the adaptation to the load tracking is likely to be minimal.

I. INTRODUCTION

Switched-mode power conversion keeps gaining momentum due to its efficiency and flexibility. An important application is ac drives where induction motors are fed by inverters so that both frequency and voltage can be finely varied. Two major approaches exist, relying on Pulse Width Modulation (PWM) or Pulse Density Modulation (PDM).

In PWM, frequency and voltage control is achieved by varying the duty ratio of the inverter switches [1]. To this aim, a fixed frame frequency f_{PWM} is established, so that the time axis is divided in frame intervals. For each interval, the modulator produces a pulse, selecting its width as needed. Conversely, in PDM voltage and frequency are controlled by varying the concentration of pulses [2]. There is no frame concept, but a thin pulse duration T is established, so that the time axis is divided in pulse intervals. As time flows, for each pulse interval the modulator can decide whether to generate a pulse or not, thus varying the output density as needed.

While effective, PWM is sometimes criticized for its fixed frame frequency that may lead to evident harmonic clusters [3] in voltage and current spectra. This may cause Electro-Magnetic Interference (EMI) or acoustic noise [4]. Randomized schemes, where either the pulse width, position or frame frequency are

perturbed may reduce this effect [5]–[7]. Yet, they may lead to other issues and certainly increase system complexity.

This is one of the reasons why PDM, is now actively investigated as a PWM substitute [2]. Lacking a frame structure, it can be inherently more compliant to EMI regulations. Furthermore, the higher apparent complication of PDM is often a myth. First of all, very practical implementations now exist, typically relying on $\Delta\Sigma$ modulation [8], at times practiced with specialized quantizers (e.g., hexagonal [9] or vector type [2]). Secondly, the perception of complication mostly arises from the much wider set of tuning options that it offers. Operating in a wider design space is obviously harder. This is evident just by looking at the number of *adjustable knobs*. In PWM only the frame frequency and resolution need to be set. In $\Delta\Sigma$ modulation, which is already a special, restricted kind of PDM, the full set of coefficients for the filters inside the modulator is to be chosen by the designer, in addition to the sample rate.

In this paper we deal with this extra flexibility and its exploitation. Particularly, we try to answer a specific question. For a $\Delta\Sigma$ modulator used to drive an ac motor, there is an obvious desire to set its parameters according to the specifications of the power bridge, the motor itself and any other elements sitting between the two (e.g., a passive filter) i.e., to *adapt* the modulator to the rest of the drive. Now, given that the motor behavior can vary, even significantly, with the mechanical load applied to its shaft, should one try to track these changes, making the modulator parameters vary accordingly? Or would this be a useless attempt at over optimize the system, with negligible benefit in terms of measured performance?

To answer this question we simulate a realistic motor, modeled at different loading conditions and with bridge commands synthesized by different $\Delta\Sigma$ modulators, some of which explicitly designed after the motor behavior at a specific mechanical loading. For the modulator optimization we exploit a recent result that enables its adaptation to the user of the $\Delta\Sigma$ streams [10], [11]. Eventually, for each loading condition, we compare the optimal behavior with that obtained from the modulator optimized at another operating condition.

II. MODELING

In our analysis, we exploit a realistic motor model. Yet, we consider an idealized setup restricted to a single phase feed-forward control as in Fig. 1. This is to decouple the matter

This is a pre-print version of a paper published in the Proceedings of 2012 IEEE International Conference on Electronics, Circuits, and Systems (ICECS). Available through DOI [10.1109/ICECS.2012.6463619](https://doi.org/10.1109/ICECS.2012.6463619). Always cite as the published version.

Copyright © 2012 IEEE. Personal use of this material is permitted. However, permission to use this material for any other purposes must be obtained from the IEEE by sending a request to pubs-permissions@ieee.org.

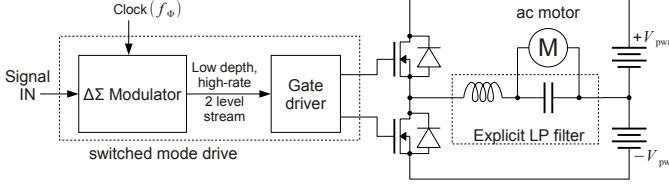


Figure 1. Idealized, single phase simulation setup.

under exam from any other second order effect, such as those possibly arising from multiphase/multilevel quantization or feed-back. We also practice a direct connection between the power bridge and the motor (i.e, we remove the filter from the architecture in Fig. 1), leaving all the signal smoothing to the reactive effects provided by the motor itself. While this is unusual for large drives, it lets the consequences of impedance variations associated to changes in the mechanical load be more evident, avoiding their hiding behind other large, fixed reactive effects.

For what concerns the electric machine, we start from the usual equations for a 3-phase induction motor. Under the basic hypothesis of writing the equations: (i) in a stationary reference frame; (ii) assuming null rotor voltages; and (iii) taking the equivalent dq -axis representation, the following differential system is derived [12]

$$\begin{aligned} \frac{di_{sd}}{dt} &= \frac{-R_s i_{sd} + \frac{\omega_m P L_m^2}{2 L_r} i_{sq} + \frac{R_r L_m}{L_r} i_{rd} + \frac{\omega_m P L_m}{2} i_{rq} + v_{sd}}{\Delta \cdot L_s} \\ \frac{di_{sq}}{dt} &= \frac{-\frac{\omega_m P L_m^2}{2 L_r} i_{sd} - R_s i_{sq} - \frac{\omega_m P L_m}{2} i_{rd} + \frac{R_r L_m}{L_r} i_{rq} + v_{sq}}{\Delta \cdot L_s} \\ \frac{di_{rd}}{dt} &= \frac{\frac{R_s L_m}{L_s} i_{sd} - \frac{\omega_m P L_m}{2} i_{sq} - R_r i_{rd} - \frac{\omega_m P L_r}{2} i_{rq} - \frac{L_m}{L_s} v_{sd}}{\Delta \cdot L_r} \\ \frac{di_{rq}}{dt} &= \frac{\frac{\omega_m P L_m}{2} i_{sd} + \frac{R_s L_m}{L_s} i_{sq} + \frac{\omega_m P L_r}{2} i_{rd} - R_r i_{rq} - \frac{L_m}{L_s} v_{sq}}{\Delta \cdot L_r} \\ \frac{d\omega_m}{dt} &= \frac{\frac{3}{4} (i_{sq} i_{rd} - i_{sd} i_{rq}) P L_m - \Lambda(t) - B \omega_m}{J}. \end{aligned} \quad (1)$$

where: $\Delta = 1 - L_m^2 / (L_s L_r)$, $i_{\alpha, \beta}$ and $v_{\alpha, \beta}$ are the currents and voltages referred to the motor stator or rotor (if $\alpha = s$ or $\alpha = r$, respectively), once projected on the β -axis for $\beta \in \{d, q\}$; ω_m is the rotor mechanical angular speed; $\Lambda(t)$ is a time-varying load. Other parameters and symbols are explained in Tbl. I that also reports the values used for simulation (which are the same used in [13], for the sake of an easy confrontation).

Evidently: (i) the model is non-linear; and (ii) it depends on the load Λ . For what concerns the first point, it is worth observing that if ω_m has an almost constant value, one can approximate away the non-linearity, obtaining the well known *linear* model describing the steady-state dynamics of the motor working at the $\omega_e = \omega_m P/2$ rotor constant electrical angular frequency. This is related to the angular frequency $\omega_w = 2\pi f_w$ of the three-phase sinusoidal drive voltage (with amplitude V_w) through the slip coefficient $\sigma = 1 - \omega_e / \omega_w$ running from 0 (no-load condition) to 1 (blocked rotor). From this linear model, one can eventually compute the admittances from each of the three phase stator voltages to the corresponding phase

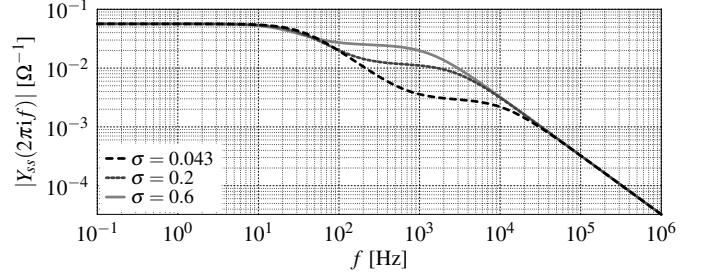


Figure 2. Transfer function due to the motor admittance at different slip values.

stator current, namely

$$Y_{ss}(i\omega) = \frac{\frac{R_r}{L_s L_r} + i \frac{\sigma}{L_s} \omega}{\frac{R_r R_s}{L_r L_s} + i (\frac{R_r}{L_r} + \sigma \frac{R_s}{L_s}) \omega - \sigma \Delta \omega^2}. \quad (2)$$

Interestingly, in this linearized model, the mechanical loading effects seem to disappear. As a matter of fact, they do not. They are only hidden inside the slip parameter. A higher load requires a higher motor torque that can only be obtained by augmenting the motor currents or accepting a higher slip. Fig. 2 shows the frequency response associated to $Y(i2\pi f)$ for three different slip values (self-friction, $\sigma = 0.043$, nominal slip $\sigma = 0.2$ and large slip $\sigma = 0.6$) and for the motor parameters in Tbl. I. Evidently, the change is quite significant. It is worth underlining that this behavior, with a pole-zero couple that moves as σ is increased, is not limited to the example setup, but rather typical.

The linearized model (2) enables a rapid evaluation of some aspects of the switched drive performance. Specifically, it lets one foresee the deviation of the motor windings currents from ideal sine waves. Such deviation results in high frequency components and on EMI. Furthermore, since currents are ultimately responsible for the motor torque, it may cause torque fluctuation, vibration and noise. Consequently, conformance of the winding currents to expected sinusoidal profiles, quantified through SNR, can be taken as an important quality figure. Formally, SNR is defined as I_N^2 / I_S^2 , where I_S is the effective value of the ideal drive and I_N is the rms current value

Table I
AC MOTOR PARAMETERS AND VALUES USED IN SIMULATION

P	4	Number of motor poles
B	$25 \cdot 10^{-3} \text{ N m s}$	Damping constant (dissipation due to windage and friction)
J	$25 \cdot 10^{-3} \text{ kg m}^2$	Moment of inertia
R_s	17.7Ω	Stator dissipative effects
R_r	13.8Ω	Rotor dissipative effects
L_s	$459.2 \cdot 10^{-3} \text{ H}$	Total 3-phase stator inductance
L_r	$457.0 \cdot 10^{-3} \text{ H}$	Total 3-phase rotor inductance
L_m	$442.5 \cdot 10^{-3} \text{ H}$	Magnetizing inductance
f_w	50 Hz	Nominal driving voltage angular frequency
V_w	320 V	Nominal driving voltage peak amplitude

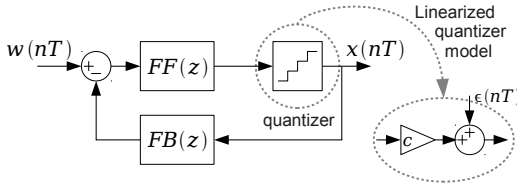


Figure 3. $\Delta\Sigma$ modulator and its approximated linear model.

associated to the switched actuation artifacts. One has

$$I_N^2 = \int_0^\infty \Psi_N^2(i2\pi f) |Y(i2\pi f)|^2 df \quad (3)$$

where $\Psi^2(i2\pi f)$ is the spectral density associated to the actuation artifacts on the voltage drive. Obviously, in Eqn. (3) there may be an additional multiplicative term $|G(i2\pi f)|^2$ whenever a filter $G(s)$ is used to feed the motor, but we have chosen not to implement it. From Eqn. (3), the importance of $Y(i2\pi f)$ is self evident, given that $\Psi^2(i2\pi f)$ depends and can be determined from the drive.

III. $\Delta\Sigma$ MODULATOR IN THE DRIVE

One of the advantages of using a $\Delta\Sigma$ modulator in the drive is to exploit its noise shaping abilities adapting them to the signals to be actuated and possibly to the drive chain. Recall that a $\Delta\Sigma$ modulator can be modeled by the standard architecture in Fig. 3, where T is the sample time. For an approximated analysis, the model gets linearized as illustrated in the circle. In this case, one can identify a Noise Transfer Function (NTF), $NTF(z)$ from the quantization noise $\epsilon(nT)$ to the output and a Signal Transfer Function (STF), $STF(z)$ from the modulator input $w(nT)$ to the output. Once the STF is taken to be unitary as it is normally the case, the modulator filters $FF(z)$ and $FB(z)$ can be designed to obtain a desired NTF as long as some constraints on the NTF itself are respected [8].

This is particularly interesting with reference to Eqn. (3). In fact, for a correctly operating modulator, $\epsilon(nT)$ can be assumed to be approximately uncorrelated to the input, white, and uniformly distributed within $[-\Delta/2, \Delta/2]$ where Δ is the quantization step [8]. Consequently, $\Psi^2(i2\pi f)$ in (3) happens to be known and approximately equal to $\frac{\Delta^2}{12} \text{sinc}^2(fT) \left| NTF\left(e^{i2\pi \frac{f}{f_s}}\right) \right|^2$, where the usual $z \leftrightarrow e^{i2\pi \frac{f}{f_s}}$ substitution is adopted, $f_s = 1/T$, a zero-order hold is assumed at the modulator output, and sinc indicates the normalized function $\sin(\pi x)/(\pi x)$. Hence, I_N^2 is

$$I_N^2 = \frac{\Delta^2}{12} \int_0^\infty \text{sinc}^2(fT) \left| NTF\left(e^{i2\pi \frac{f}{f_s}}\right) \right|^2 |Y(i2\pi f)|^2 df. \quad (4)$$

From Eqn. (4), the opportunity of optimizing $NTF(z)$ adapting it to the motor transfer function $Y(s)$ is quite evident. Thus, the following questions arise: (i) is it worth selecting a *custom* NTF rather than using a conventional design? (ii) does it make sense to continuously modify the NTF to track the variations of $Y(i2\pi f)$ due to slip changes?

To ease the answer, one may first observe that thanks to the low pass nature of $Y(i2\pi f)$, and as long as the modulator sample frequency f_s is sufficiently high, the integral in Eqn. (4) can safely be approximated as

$$I_N^2 = \frac{\Delta^2}{12\pi} \int_0^\pi |NTF(e^{i\omega})|^2 \left| \hat{Y}(e^{i\omega}) \right|^2 d\omega. \quad (5)$$

where $\hat{Y}(z)$ is a discrete time version of $Y(s)$. Then, it is worth noting, that due to the specific constraints posed by the modulator architecture, the integral cannot be minimized in *naive* ways by nullifying the NTF or by making it capable of concentrating *all* the quantization noise at the single frequency where $\hat{Y}(e^{i\omega})$ attenuates most. Conversely, as explained in [8], one needs to assure that $|NTF(e^{i\omega})|$ never exceeds certain values, is non-negligible in sufficiently large intervals and is realized by some $NTF(z)$ whose impulse response has a unitary first coefficient [8]. Intuitively, in presence of such constraints, the integral can be reduced by taking $|NTF(e^{i\omega})|$ to be approximately the *inverse* of $|\hat{Y}(z)|$, as discussed in [14]. This may require some manual adjustment to obtain a stable $NTF(z)$. Then, further adjustment may be required on gain and range (namely the difference between maximum and minimum gain values) to satisfy the modulator requirements. Alternatively, one can choose the method in [10], [11] to directly obtain a suitable $NTF(z)$ through a better formalized path.

Following one of the two approaches above, one may obtain different NTFs matched to specific slip values. These can be checked against a conventional NTF using expression (5) to evaluate the convenience of custom NTFs over conventional ones. Furthermore, one can evaluate some custom NTFs designed for different slip values one against the other to see the convenience of tracking slip changes by a continuous NTF adjustment.

IV. EXPERIMENTAL RESULTS

In our experiments, we refer to the parameter set in Tbl. I. Furthermore, we assume that the actuation frequency is comprised in a [0-50]Hz interval. Finally, for the $\Delta\Sigma$ modulator we take an over-sample rate (OSR) equal to 1000, setting the sample frequency at 100 kHz.

With this, the diagram in Fig. 4 shows a standard NTF obtained for a 4th order modulator through the popular design assistant DELSIG [15], together with three NTFs optimized for the same slip values used for Fig. 2. These are 8th order and obtained following [10], [11]. The comparison of NTFs corresponding to different modulator orders should not appear unfair, since: (i) conventional methodologies cannot safely go beyond order 4 for this setup; and (ii) the difference between the NTFs in the two diagram is mostly due to the different design methodology rather than the different order. Indeed, the striking contrast between the diagrams owes to the fact that conventional methodologies are only based on the OSR, while the other NTFs also explicitly take into account the need to reduce the value of expression (5).

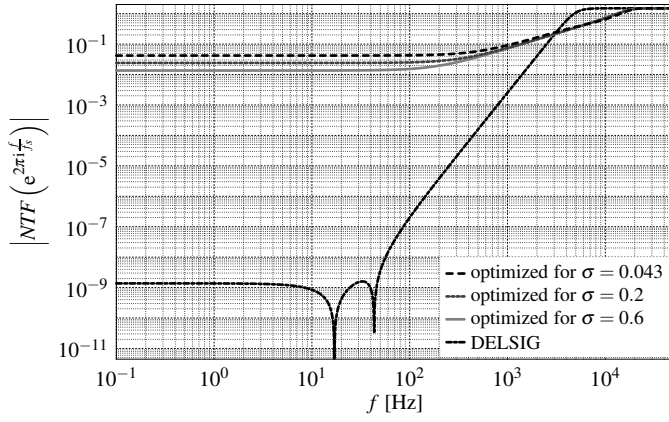


Figure 4. Conventional (DELSIG) NTF and NTFs optimized at specific motor loads and slips.

Table II

SNR IN DB OBTAINED USING THE VARIOUS NTFs IN COMBINATION WITH THE MOTOR AT DIFFERENT MECHANICAL LOAD AND SLIP CONDITIONS. DATA OBTAINED FROM EQN. (5).

	Mechanical Loading Condition		
	$\sigma = 0.043$	$\sigma = 0.2$	$\sigma = 0.6$
Standard NTF	24.72 ✗	29.48 ✗	35.13 ✗
NTF optimized for $\sigma = 0.043$	29.60 ✓	33.98	39.39
NTF optimized for $\sigma = 0.2$	29.50	34.11 ✓	39.64
NTF optimized for $\sigma = 0.6$	29.45	34.09	39.67 ✓

The effectiveness of the various NTFs is reported in Tbl. II which shows the SNR obtained from Eqn. (5), considering the motor model at the various slip conditions. Data has been obtained selecting a 50 Hz operation at 60 % of the motor nominal voltage (namely 190 V peak).

From the tabled data, a well perceivable advantage, quantifiable in approximately 3-5 dB (i.e. an approximate halving of the noise), seems to be achievable by using an NTF designed in accordance to the motor model (rows 2 to 4), with respect to a standard NTF designed considering the OSR only (row 1). Furthermore, considering rows 2 to 4, note that in each column the best value can always be found on the diagonal. In other words, and not surprisingly, the best performance at any slip condition appears to be obtainable using the NTF designed according to the motor admittance at that particular slip condition. Nonetheless, the advantage that the best setup offers over the others looks minimal. This indicates that optimizing the NTF for a specific slip may not be truly convenient. Indeed, such a conclusion could already be expected from the curves in Fig. 4, where the optimized NTF does not change much by changing the slip level for which the optimization is done.

To be extremely scrupulous, one may want not to limit the analysis to data obtained by Eqn. (5), due to the many approximations practiced to achieve such model. These basically amount to the linearization of both the motor and the modulator models. Among the two, the second one is certainly the most critical. Thus, it is worth repeating the test by means of a

Table III

SNR IN DB OBTAINED USING THE VARIOUS NTFs IN COMBINATION WITH THE MOTOR AT DIFFERENT MECHANICAL LOAD AND SLIP CONDITIONS. DATA OBTAINED FROM TIME DOMAIN SIMULATIONS WITH A NONLINEAR MODULATOR MODEL AND A LINEARIZED MOTOR MODEL.

	Mechanical Loading Condition		
	$\sigma = 0.043$	$\sigma = 0.2$	$\sigma = 0.6$
Standard NTF	25.87 ✗	30.73 ✗	36.39
NTF optimized for $\sigma = 0.043$	28.04	31.97	35.39 ✗
NTF optimized for $\sigma = 0.2$	28.16	32.67	37.18
NTF optimized for $\sigma = 0.6$	28.26 ✓	33.01 ✓	38.21 ✓

time domain simulation of the modulator, based on a realistic quantizer. This new data is illustrated in Tbl III and is in good accordance to the previous one. Variations are typically within 1-1.5 dB. This indicates that the nonlinear effects in the modulator should not be ignored, though. Altogether, we have a confirmation that it is advantageous to design the NTF taking into account the motor model, even if the more realistic simulations cause the gap over a conventional NTF to shrink to approximately 2.5 dB. This is still a 44 % reduction in noise. Furthermore, the new test reveals that the data fluctuations due to the nonlinear effects break the already thin advantage related to optimizing the NTF for some specific slip level. Indeed, in the current table, the optimal values for each column do not lay anymore on the diagonal of rows 2 to 4. This confirms that trying to track a specific slip level with the NTF is a useless over-optimization.

V. CONCLUSIONS

We have considered the use of $\Delta\Sigma$ modulators in switched mode drives for ac motors. Specifically, we have looked at how the modulator NTF should be designed to achieve the best possible performance, trying to see if an NTF design practiced taking into account the motor model and the motor loading condition can be advantageous. From the proposed analysis, it appears that designing the NTF in accordance to the motor model can be convenient, while trying to have an NTF actively tracking the motor slip condition is probably over-engineering. From our analysis, designing the NTF at a single, large slip condition is enough to capitalize some non-negligible advantage (an over 40 % reduction of the quantization noise effect over the motor winding currents). Clearly, the proposed analysis is based on simulation and limited to the parameter set of a specific motor. However, we expect our conclusions to be valid for many similar setups.

REFERENCES

- [1] D. G. Holmes and T. A. Lipo, *Pulse Width Modulation for Power Converters*. IEEE Press, 2003.
- [2] B. Jacob and M. R. Baiju, "Spread spectrum modulation scheme for two-level inverter using vector quantised space vector-based pulse density modulation," *IET Electrical Power Application*, vol. 5, no. 7, pp. 589–596, 2011.
- [3] J. T. Boys and P. G. Handley, "Harmonic analysis of space vector modulated PWM waveforms," *Electric Power Applications, IEE Proceedings B*, vol. 137, no. 4, pp. 197–204, 1990.

- [4] T. F. Lowery and D. W. Petro, "Application considerations for PWM inverter-fed low-voltage induction motors," *IEEE Trans. Ind. Appl.*, vol. 30, no. 2, pp. 286–293, 1994.
- [5] A. M. Stanković and H. Lev-Ari, "Randomized modulation in power electronic converter," *Proceedings of the IEEE*, vol. 90, no. 5, pp. 782–799, May 2002.
- [6] M. Balestra, A. Bellini, C. Callegari, R. Rovatti, and G. Setti, "Chaos-based generation of PWM-like signals for low-EMI induction motor drives: Analysis and experimental results," *IEICE Transactions on Electronics*, vol. E87-C, no. 1, pp. 66–75, Jan. 2004.
- [7] S. Callegari, R. Rovatti, and G. Setti, "Chaotic modulations can outperform random ones in EMI reduction tasks," *Electronics Letters*, vol. 38, no. 12, pp. 543–544, Jun. 2002.
- [8] R. Schreier and G. C. Temes, *Understanding Delta-Sigma Data Converters*. Wiley-IEEE Press, 2004.
- [9] G. Luckjiff and I. Dobson, "Hexagonal Sigma-Delta modulation," *IEEE Trans. Circuits Syst. I*, vol. 50, no. 8, Aug. 2003.
- [10] S. Callegari and F. Bizzarri, "Output filter aware optimization of the noise shaping properties of $\Delta\Sigma$ modulators via semi-definite programming," *IEEE Trans. Circuits Syst. I* submitted, 2012.
- [11] S. Callegari, "An alternative strategy for optimizing the noise transfer function of $\Delta\Sigma$ modulators," ARCES, University of Bologna, Internal Report, 2012.
- [12] A. E. Fitzgerald, C. Kingsley, Jr., and A. Kusko, *Electrical Machinery*. McGraw Hill, 1990.
- [13] F. Bizzarri, S. Callegari, and G. Gruosso, "Towards a nearly optimal synthesis of power bridge commands in the driving of AC motors," in *Proceedings of ISCAS 2012*, Seoul, May 2012.
- [14] S. Callegari, F. Bizzarri, R. Rovatti, and G. Setti, "On the approximate solution of a class of large discrete quadratic programming problems by $\Delta\Sigma$ modulation: the case of circulant quadratic forms," *IEEE Trans. Signal Process.*, vol. 58, no. 12, pp. 6126–6139, Dec. 2010.
- [15] R. Schreier, *The Delta-Sigma Toolbox*, Analog Devices, 2011, release 7.4, also known as "DELSIG". [Online]. Available: <http://www.mathworks.com/matlabcentral/fileexchange/>